Sampled-Data System Analysis of Antenna Conical-Scan Tracking

R. A. Winkelstein
Communications Systems Research Section

The conical-scan tracking system described by Ohlson and Reid in JPL Technical Report 32-1605 is analyzed as a sampled-data feedback control system. Tracking mode equations for both spacecraft signals and radio source signals are developed. In the case of spacecraft tracking, a rationale is presented for selection of parameters which minimizes the sum of the required scan radius and three times the RMS error jitter. With this criterion, reasonable system performance can be obtained with signals down to receiver threshold. For radio source tracking, the RMS error jitter is negligible, and a set of system parameters is recommended which allows conservative operation of the system.

I. Introduction

Conical-scan tracking is a method for automatically tracking a signal source with a Deep Space Network (DSN) antenna by continuously rotating the antenna a small fraction of the antenna beam width around the tracking boresight, a hypothetical line between the antenna and signal source. An error in the tracking angle results in a systematic variation in received signal strength which is used to derive correction offsets in the two antenna pointing axes. The DSN has used conical-scan tracking for several years, and an excellent report (Ref. 1.) has been written by J. E. Ohlson and M. S. Reid describing the system both theoretically and practically. Using Ohlson's work as a guide, the following report recasts the description of the conical-scan system into that of a sampled-data feedback control system with parameters perhaps more familiar to the control system analyst. In addition, a rationale is presented for optimum selection of system parameters as a function of desired system performance. Theoretical results derived from the sampled-data system model are in complete agreement with Ref. 1., and a correspondence of selected parameters is listed in Appendix B.

II. System Description

A block diagram of the conical-scan system is shown in Fig. 1. Two feedback channels are used, one for an assumed elevation axis correction and the other for an assumed cross-elevation axis correction. Both channels are identical except for the quadrature references, $\sin \omega_m t$ and $\cos \omega_m t$, and any necessary trigonometric transformations relating the assumed axes with the actual antenna axes driven by the antenna pointing subsystem. The radian rotation frequency, ω_m, is given by

$$\omega_m = \frac{2\pi}{P(1 - A)} \tag{1}$$

where $P(1 - A)$ is the rotation period of the antenna, typically 28 seconds. After each rotation, the antenna is stopped rotating for "AP" seconds, usually two, during which time new offset corrections are calculated and the antenna slightly repositioned as a result. Thus P represents the total time

between successive corrections, and is the basic timing quantity for the sampled-data model.

The receiver generates a signal strength voltage sampled at ten times a second by the correlator. Two types of signals can be tracked with the conical-scan system. One type is a spacecraft signal, in which case the signal strength voltage is derived from the receiver automatic gain control (AGC) circuit. The second signal type comes from a wide band stellar radio source. In this case, the signal strength voltage comes from a wide band power detector.

The correlator block provides an estimate of the offset error by correlating the sampled signal strength voltage against the correlator input reference. An updated estimate is obtained for each rotation of the antenna. These estimates are filtered by the digital filter according to the relation

$$X_3(k) = X_3(k - 1) + k_d X_2(k) \tag{2}$$

where $X_3(k)$ is the kth filter output, $X_3(k - 1)$ is the previous filter output, $X_2(k)$ is the kth filter input, and k_d is a gain constant. The antenna pointing subsystem provides a constant offset proportional to X_3 for each channel throughout the succeeding rotation period. In addition to these fixed offsets and the conical-scan rotation signals, the antenna pointing subsystem provides position and velocity correction signals from predicted information called predicts which are generated external to the system before the track. Predicts are required by the conical-scan system because the system using Eq. (2) is a first order system that can only correct for small fixed offsets in the predict values. In this sense, the conical-scan system is used only to "fine tune" the pointing angle generated by the predicts.

III. System Analysis

In a properly operating conical-scan tracking system, the two feedback channels are identical but independent. Therefore an analysis will be made only of the elevation channel, with similar results applicable to the cross-elevation channel.

A. Laplace Block Diagram

A first step in the analysis is a formulation of the Laplace block diagram as shown in Fig. 2. $\phi(s)$ is the Laplace transform of the desired elevation angle, and $C(s)$ is the Laplace transform of the elevation angle generated by the conical-scan system. "s" is the Laplace transform complex frequency. The channel error, $E(s)$, given by

$$E(s) = \phi(s) - C(s) \tag{3}$$

is input to the correlator which acts as an integrate-and-dump circuit.

The correlator circuit can be represented as a pure integrator whose output is the difference between the present value and a past value occurring at the start of the integration time. This past value is obtained through a pure delay, $e^{-sP(1-A)}$, where e is the natural logarithm base, and $P(1 - A)$ is as defined in Eq. (1). "k_i", the integrator gain constant, is a function of the signal type received, and includes several receiver parameters. Detailed derivations of k_i for both spacecraft and radio source signals will be made in later sections. The Z-transform, (Ref. 2), of the correlator output, $X_2(z)$, is the sum of the error estimate, $X_1(z)$, and a noise value, $N(z)$, generated by the receiver noise processes. z is equal to e^{sP}. $N(z)$ will be determined in later sections of this report, but in this section it will be considered as an input quantity.

The transmission function shown for the digital filter in Fig. 2 results from taking the Z-transform of Eq. (2). Since the offset correction calculated by the digital filter is maintained as a constant value, $C(s)$, throughout the antenna rotation period, the resulting model for this operation is known as a zero-order hold circuit with a gain constant of k_h as shown in Fig. 2.

B. Z-transform Equations

An analysis of the conical-scan sampled-data channel of Fig. 2 will be carried out in the z complex plane. It is desired to determine $E(z)$, the Z-transform of $E(s)$, as a function of the input and noise signals. The procedure is to take the Z-transform of the state equations of Fig. 2 and then generate the signal flow graph of Fig. 3. $E(z)$ is then calculated by means of Mason's general gain formula (Ref. 3). The relevant state equations for Fig. 2 are

$$E(s) = \phi(s) - X_3(z)\frac{z - 1}{z}\frac{k_h}{s} \tag{4}$$

$$X_1(s) = \left(k_i \frac{\phi(s)}{s} - X_3(z)\, k_h k_i \frac{z - 1}{z}\frac{1}{s^2}\right)\left(1 - e^{-sP(1-A)}\right) \tag{5}$$

$$X_2(z) = X_1(z) + N(z) \tag{6}$$

$$X_3(z) = X_2(z)\, k_d \frac{z}{z - 1} \tag{7}$$

Taking the Z-transform of Eqs. (4) and (5) respectively gives

$$E(z) = \phi(z) - X_3(z)\, k_h \tag{8}$$

$$X_1(z) = k_i\left[\mathcal{Z}\left(\frac{\phi(s)}{s}\right) - \mathcal{Z}_m\left(\frac{\phi(s)}{s}\right)_{m=A}\right]$$

$$- X_3(z)\, k_h k_i P(1 - A)\frac{1}{z} \tag{9}$$

where $\mathcal{Z}(\phi(s)/s)$ is the Z-transform of $\phi(s)/s$, and $\mathcal{Z}_m(\phi/s)_{m=A}$ is the modified Z-transform of $\phi(s)/s$, with "A" substituted for the parameter "m". This latter expression results from the standard technique of using the modified Z-transform to find the Z-transform of a function with pure delay.

Eqs. (6) through (9) form the signal flow graph of Fig. 3, from which $E(z)$ is found to be

$$E(z) = \phi(z) - \frac{\left[\mathcal{Z}\left(\frac{\phi(s)}{s}\right) - \mathcal{Z}_m\left(\frac{\phi(s)}{s}\right)_{m=A}\right]k_i k_d k_h\, Z}{z - 1 + k_T}$$

$$- \frac{N(z)k_h k_d\, Z}{z - 1 + k_T} \tag{10}$$

$$k_T = k_i k_d k_h\, P(1 - A) \tag{11}$$

where k_T is the overall loop gain constant. The response to a constant step input, ϕ_c, is next found with $N(z)$ set equal to zero. For a constant step input

$$\phi(s) = \frac{\phi_c}{s} \tag{12}$$

$$\phi(z) = \frac{\phi_c z}{z - 1} \tag{13}$$

$$\mathcal{Z}\left(\frac{\phi(s)}{s}\right) = \frac{\phi_c P z}{(z - 1)^2} \tag{14}$$

$$\mathcal{Z}_m\left(\frac{\phi(s)}{s}\right) = \phi_c\left(\frac{AP}{z - 1} + \frac{P}{(z - 1)^2}\right) \tag{15}$$

Using the values from Eqs. (12) through (15) gives

$$E(z) = \frac{\phi_c z}{z - 1 + k_T} \tag{16}$$

and taking the inverse Z-transform of Eq. (16) gives

$$E_k = \phi_c(1 - k_T)^k \tag{17}$$

where E_k is the loop error after the kth period P of the input step. Eq. (17) shows that the loop error is driven to zero when the input signal is a constant step offset.

A system response time constant, τ, may be defined by using the exponential equivalent to the step offset response

$$(1 - k_T)^k = e^{-(kP)/\tau} \tag{18}$$

Solving Eq. (18) for τ gives

$$\tau = \frac{-P}{ln(1 - k_T)} \tag{19}$$

τ is considered to be of prime interest to the conical-scan system user, and therefore is presented as one of the tradeoff parameters when selecting an optimum set of system constants.

C. Root Locus Analysis

Root locus theory is useful in predicting the region of feedback system stability. The root locus is a plot in the complex plane of closed loop gain poles as a function of an open loop gain constant. A sampled-data system is stable if its closed loop poles are within the unit circle in the z complex plane. From Fig. 2, the open loop gain, G_{ol}, is

$$G_{ol}(s) = -\frac{k_i k_h k_d}{s^2}\left(1 - e^{-sP(1-A)}\right) \tag{20}$$

Taking the Z-transform of Eq. (20) gives

$$G_{ol}(z) = -\frac{k_T}{z - 1} \tag{21}$$

Thus k_T is selected as the open loop gain constant of interest. The closed loop gain, G_{cl}, is

$$G_{cl}(z) = \frac{1}{1 - G_{ol}(z)} = \frac{z - 1}{z - (1 - k_T)} \tag{22}$$

From Eqs. (21) and (22) it is seen that the conical-scan channel has a single open loop pole at z equal to one. This pole travels to the left along the real axis as a closed loop pole in direct proportion to k_T. At a value of k_T equal to two, which is the upper limit for system stability, the closed loop pole leaves the unit circle. This result is in agreement with Eq. (17) which shows an increasing error for k_T greater than two.

Also predicted by root locus theory is that a sampled-data feedback system with only a single pole at z equal to one will have a steady state error to a ramp or velocity input. This then is the reason for the requirement on the predicts to compensate for the velocity and higher degree components of the pointing axis angle motion.

D. System Noise Gain

As shown in Fig. 3, system generated noise, $N(z)$, acts as an input to the channel loop and causes the loop error, $E(z)$, to jitter. The root mean square (RMS) value of the output jitter, σ_E, is proportional to σ_N, the RMS value of $N(z)$. Setting $\phi(s)$ equal to zero in Eq. (10) gives

$$E(z) = - \frac{N(z)\, k_h k_d\, z}{z - 1 + k_T} \tag{23}$$

The sampled-data power spectrum (Ref. 4) of $E(z)$ is $\Phi_E(z)$ and is given by

$$\Phi_E(z) = \left\langle E(z^{-1})\, E(z) \right\rangle = - \frac{\Phi_N(z)\, k_h^2 k_d^2\, z}{(1 - k_T)\left(z - \dfrac{1}{1 - k_T}\right)(z - 1 + k_T)} \tag{24}$$

where $\Phi_N(z)$, the power spectrum of $N(z)$, is

$$\Phi_N(z) = \left\langle N(z^{-1})\, N(z) \right\rangle \tag{25}$$

Braces indicate ensemble average. For independent noise samples of $N(z)$, the sampled-data autocorrelation function, $\beta_N(kP)$, of $N(z)$ is

$$\beta_N(kP) = \begin{cases} \sigma_N^2 & k = 0 \\ 0 & k \neq 0 \end{cases} \tag{26}$$

The sampled-data power spectrum $\Phi_N(z)$ of $N(z)$ is the two-sided Z-transform of $\beta_N(kP)$. Therefore $\Phi_N(z)$ is

$$\Phi_N(z) = \sum_{k=-\infty}^{\infty} \beta_N(kP)\, z^{-k} = \sigma_N^2 \tag{27}$$

Eq. (24) becomes

$$\Phi_E(z) = - \frac{\sigma_N^2 k_h^2 k_d^2\, z}{(1 - k_T)\left(z - \dfrac{1}{1 - k_T}\right)(z - 1 + k_T)} \tag{28}$$

The inverse Z-transform of $\Phi_E(z)$ is

$$\beta_E(kP) = \frac{1}{2\pi i} \oint dz\; \Phi_E(z)\, z^{k-1} \tag{29}$$

where the path of integration in the Z complex plane is counterclockwise on the unit circle, and i is the positive square root of minus one. $\beta_E(kP)$ is the sampled-data autocorrelation function of $E(z)$, and kP is correlation lag time. σ_E^2 is found from

$$\sigma_E^2 = \beta_E(0) = \frac{1}{2\pi i} \oint \frac{dz}{z}\, \Phi_E(z) \tag{30}$$

Substituting Eq. (28) into Eq. (30), and using the method of residues about the pole z equal to $1 - k_T$ gives

$$\sigma_E = \frac{\sigma_N}{k_i P(1 - A)} \sqrt{\frac{k_T}{2 - k_T}} \tag{31}$$

In agreement with root locus theory, and the response found for a step input, it is seen that the jitter on $E(z)$ becomes infinite as k_T approaches the value of two. Actual

selection of system parameters depends upon the specific relationship of k_i and σ_N to the receiving system being used.

IV. Spacecraft Tracking Correlation

A. Derivation of Equations

A simplified block diagram of the spacecraft tracking receiver system is shown in Fig. 4. The carrier, E_{ca}, of the spacecraft signal impinges on the DSN antenna with a value of

$$E_{ca} = \sqrt{2P_s} \cos \omega_0 t \tag{32}$$

where P_s is the power in the carrier, and ω_0 is the carrier radian frequency. The antenna has a power gain, G_p, given by

$$G_p = \left(\frac{1}{16}\right)^{\psi^2/W^2} \tag{33}$$

where ψ is the angle in degrees that the antenna points away from the tracking boresight, and W is the beamwidth in degrees between the half-power points. Thus the constant of 1/16 is chosen to give a value of 1/2 to G_p when the ratio of ψ to W is 1/2. In terms of an exponential function, Eq. (33) becomes

$$G_p = e^{-\mu(\psi^2/W^2)} \tag{34}$$

$$\mu = 4 \ln 2 \tag{35}$$

where ln is the natural logarithm. Eqs. (33), (34), and (35) assume a circular antenna pattern.

At point "a" of Fig. 4, the voltage V_a is

$$V_a(t) = E_a(t) + n_a(t) \tag{36}$$

$$E_a(t) = \sqrt{2P_s G_p} \cos \omega_0 t \tag{37}$$

Here, $E_a(t)$ is the signal voltage, and $n_a(t)$ is the noise voltage associated with the system temperature, T_s. $n_a(t)$ has a wide band two-sided power spectral density, $\Phi_a(\omega)$, given by

$$\Phi_a(\omega) = \frac{KT_s}{2} \tag{38}$$

where K is Boltzmann's constant equal to 1.3806×10^{-23} watt seconds/degree Kelvin. At point "b" in Fig. 4, the voltage V_b is

$$V_b(t) = E_b(t) + n_b(t) \tag{39}$$

$$E_b(t) = H\sqrt{2P_s G_p} \cos \omega_0 t \tag{40}$$

where $E_b(t)$, the signal portion of V_b, has a gain factor of H, the receiver voltage gain constant. $n_b(t)$, the noise portion of V_b, has a two-sided spectral density $\Phi_b(\omega)$ given by

$$\Phi_b(\omega) = \frac{H^2 KT_s}{2} \tag{41}$$

with a one-sided noise bandwidth of B hertz formed by the IF bandpass characteristic of the receiver. This type of noise, as derived in Appendix A of Ref. 5, can be represented as

$$n_b(t) = \sqrt{2}\,(n_1(t) \sin \omega_0 t + n_2(t) \cos \omega_0 t) \tag{42}$$

where Φ_1 and Φ_2, the power spectral densities of $n_1(t)$ and $n_2(t)$, are

$$\Phi_1(\omega) = \Phi_2(\omega) = \Phi_b(\omega) \tag{43}$$

and $n_1(t)$ and $n_2(t)$ are independent baseband signals centered about zero frequency with a two-sided bandwidth of B hertz.

At point "c" in Fig. 4, the voltage V_c becomes

$$V_c(t) = E_c(t) + n_c(t) \tag{44}$$

$$E_c(t) = 2H\sqrt{P_s G_p} \cos^2 \omega_0 t \tag{45}$$

$$n_c(t) = 2(n_1(t) \sin \omega_0 t + n_2(t) \cos \omega_0 t) \cos \omega_0 t \tag{46}$$

High order trigonometric terms in Eqs. (45) and (46) are eliminated by the low pass filter in Fig. 4, and therefore the voltage V_d at point "d" becomes

$$V_d(t) = E_d(t) + n_d(t) \tag{47}$$

$$E_d(t) = H\sqrt{P_s G_p} \tag{48}$$

$$n_d(t) = n_2(t) \tag{49}$$

where $E_d(t)$ and $n_d(t)$ are respectively the signal and noise portions of $V_d(t)$. This voltage is sampled by the antenna pointing system computer and a correlation summation is formed which closely approximates the continuous integral shown in the correlator box of Fig. 4. At the end of each period P, an estimate, X_2, of the offset error is provided such that the mean, X_1, is

$$X_1 = k_c \int_{AP}^{P} dt\, E_d(t) \sin \omega_m t \tag{50}$$

and the noise portion, N, is

$$N = k_c \int_{AP}^{P} dt\, n_d(t) \sin \omega_m t \tag{51}$$

where k_c is the correlator gain constant. The cross-elevation correlator integral would contain the terms $\cos \omega_m t$ instead of the term $\sin \omega_m t$.

B. Correlation Gain Constant

G_p in Eq. (48) is a function of time t due to the action of the conical-scan motion of the antenna. This motion produces a time variation on ψ^2 in Eq. (34) given by

$$\psi^2(t) = (\theta + R \cos \omega_m t)^2 + (\phi + R \sin \omega_m t)^2 \tag{52}$$

where θ and ϕ are respectively the cross-elevation and elevation errors, assumed constant for $AP < t < P$. $R \cos \omega_m t$ and $R \sin \omega_m t$ are the conical-scan drive equations to the assumed cross-elevation and elevation antenna pointing axes. When the offsets are zero, the scan radius R is the constant angle with which the antenna rotates about the tracking boresight. Using Eqs. (52) and (34), Eq. (48) becomes

$$E_d(t) = H\sqrt{P_s} \exp\left[-\frac{\mu}{W^2}(R^2 + \theta^2 + \phi^2 + 2R(\theta \cos \omega_m t + \phi \sin \omega_m t))\right] \tag{53}$$

From tables of integrals, Ref. 6, the following equation may be derived

$$\int_c^{c+2\pi} dx \exp(A \cos X + B \sin X) \sin X = \frac{2\pi B}{\sqrt{A^2 + B^2}} I_1\left(\sqrt{A^2 + B^2}\right) \tag{54}$$

where I_1 is the modified Bessel function of order one, and c is an arbitrary constant. Using Eqs. (53) and (54), Eq. (50) is evaluated to be

$$X_1 = -k_c H\sqrt{P_s}\, P(1 - A) \exp -\frac{1}{2W^2}\left[(R^2 + \theta^2 + \phi^2)\right] \times \frac{\phi}{\sqrt{\phi^2 + \theta^2}} I_1\left(\frac{R\mu}{W^2}\sqrt{\phi^2 + \theta^2}\right) \tag{55}$$

If the assumption is made that θ and ϕ are much smaller than R, the approximation of

$$e^{-X} \approx 1 - X \tag{56}$$

may be made to Eq. (50) before evaluation of the integral, or the approximation of

$$I_1(X) \approx \frac{X}{2} \tag{57}$$

may be made to Eq. (55). In either case, Eq. (55) simplifies to

$$X_1 = -k_c H\sqrt{P_s}\, P(1 - A) \frac{R\mu}{2W^2} \exp\left(-\frac{\mu R^2}{2W^2}\right)\phi$$

$$\phi,\ \theta \ll R \tag{58}$$

From Fig. 2, the correlator response is

$$X_1(s) = E(s)\frac{k_i}{s}\left(1 - e^{-sP(1-A)}\right) \tag{59}$$

For a constant input, $-\phi$

$$E(s) = -\frac{\phi}{s} \tag{60}$$

Therefore Eq. (59) becomes

$$X_1(s) = -\frac{\phi k_i}{s^2}\left(1 - e^{-sP(1-A)}\right) \tag{61}$$

Taking the Z-transform of Eq. (61) gives

$$X_1(Z) = -\frac{\phi k_i P(1 - A)}{z - 1} \tag{62}$$

The inverse Z-transform of Eq. (62) is

$$X_n = -\phi k_i P(1 - A) \qquad n = 1, 2, \ldots \tag{63}$$

Comparing Eqs. (58) and (63) gives the value for the correlation constant k_i.

$$k_i = k_c H \sqrt{P_s}\,\frac{R\mu}{2W^2} \exp\left(-\frac{\mu R^2}{2W^2}\right) \tag{64}$$

C. Noise Variance

The variance σ_N^2 of the noise N of Eq. (51) is

$$\sigma_N^2 = \langle N^2 \rangle \tag{65}$$

Substituting Eq. (51) into Eq. (65) gives

$$\sigma_N^2 = k_c^2 \int_{AP}^{P} dt \int_{AP-t}^{P-t} d\tau_1\, \beta_d(\tau_1) \sin \omega_m t \sin \omega_m (t + \tau_1) \tag{66}$$

where $\beta_d(\tau_1)$ is the autocorrelation of $n_d(t)$ as a function of the lag time τ_1. β_d is the inverse Fourier transform of Φ_d.

$$\beta_d(\tau_1) = \frac{1}{2\pi} \int_{-\infty}^{\infty} d\omega\, \Phi_d(\omega) \exp(i\omega\tau_1) \tag{67}$$

From Eqs. (41), (43), and (49)

$$\Phi_d(\omega) = \frac{H^2 K T_s}{2} \tag{68}$$

The bandwidth of $n_d(t)$ may be taken as infinite since Eq. (51) acts as an integrator with a resulting bandwidth much less than the B hertz specified for Eq. (41). Evaluating Eq. (67) using Eq. (68) gives

$$\beta_d(\tau_1) = \frac{H^2 K T_s}{2}\,\delta(\tau_1) \tag{69}$$

where $\delta(\tau_1)$ is the Dirac delta function, (Ref. 7). From Eqs. (66) and (69), σ_N is found to be

$$\sigma_N = \frac{k_c H}{2} \sqrt{K T_s P(1 - A)} \tag{70}$$

and therefore, Eq. (31) becomes

$$\sigma_E = \frac{W^2 \exp(\mu R^2/2W^2)}{\mu R} \sqrt{\frac{K T_s}{P_s P(1 - A)}} \sqrt{\frac{k_T}{2 - k_T}} \tag{71}$$

D. Spacecraft Correlation S-Curve

The transfer function specified by Eq. (58) is true only in the region where ϕ is close to zero. As the offset error ϕ departs from zero, a closer approximation to Eq. (55) is found by including the ϕ^2 value in the exponential term.

$$X_1 = -k_c H \sqrt{P_s} P(1 - A)\,\frac{R\mu}{2W^2} \times \exp\left(-\frac{\mu R^2}{2W^2}\right) \phi \exp\left(-\frac{\mu \phi^2}{2W^2}\right) \tag{72}$$

Normalizing Eq. (72) gives

$$y = -\frac{2X_1 W \exp(\mu R^2/2W^2)}{k_c H \sqrt{P_s} P(1 - A) R\mu} = \frac{\phi}{W} \exp\left[-\frac{\mu}{2}\left(\frac{\phi}{W}\right)^2\right] \tag{73}$$

A plot of Eq. (73) is shown in Fig. 5. Also shown in Fig. 5 are values for the slope of Y. This slope is a multiplying factor to

k_i for a large deviation of ϕ. Examination of Fig. 5 shows that the slope error is less than 20% for values of ϕ less than 0.22.

V. Selection of Parameters

In this section, a rationale will be developed for selection of parameters which will provide in a defined sense, an optimum tradeoff between the system time constant τ, and the scan radius R. R results in a loss of signal strength called crossover loss due to the fact that the antenna is pointing R degrees away from the target. This loss is the value of G_p when R is substituted for ψ in Eq. (34). Thus the crossover loss, C_L, in dB is given by

$$C_L = \left(\frac{R}{W}\right)^2 40 \log_{10} 2 \tag{74}$$

Normally it is desirable for C_L to be in the order of 0.1 dB. Increasing the value of R will result in excessive crossover loss. However, Eq. (71) shows that for weak signal levels, low values of R will result in excessive jitter in the error. If some function, $F(R/W)$, can be found which combines the effects of both crossover loss and error jitter, then an optimum R can be determined which will minimize F. A recommended function for this purpose is

$$F\left(\frac{R}{W}\right) = \frac{R}{W} + 3\frac{\sigma_E}{W} \tag{75}$$

Thus, statistically speaking, the antenna pointing loss for both R and error jitter will be less than F for 99.7% of the time. Using Eq. (71), Eq. (75) and its derivative become

$$F\left(\frac{R}{W}\right) = \frac{R}{W} + \frac{D \exp\left[\frac{\mu}{2}\left(\frac{R}{W}\right)^2\right]}{\frac{R}{W}} \tag{76}$$

$$F'\left(\frac{R}{W}\right) = 1 + \frac{D \exp\left[\frac{\mu}{2}\left(\frac{R}{W}\right)^2\right]\left[\mu\left(\frac{R}{W}\right)^2 - 1\right]}{\left(\frac{R}{W}\right)^2} \tag{77}$$

$$D = \frac{3}{\mu}\sqrt{\frac{KT_s}{P_s P(1-A)}}\sqrt{\frac{k_T}{2-k_T}} \tag{78}$$

Solving for F and D in Eqs. (76) and (77) gives the minimum value of F and the optimum value of D as a function of R.

$$F\left(\frac{R}{W}\right) = \frac{R}{W}\left(1 + \frac{1}{1-\mu\left(\frac{R}{W}\right)^2}\right) \tag{79}$$

$$D = \frac{\left(\frac{R}{W}\right)^2 \exp\left[-\frac{\mu}{2}\left(\frac{R}{W}\right)^2\right]}{1-\mu\left(\frac{R}{W}\right)^2} \tag{80}$$

For selected values of T_s, P_s, P, and A, the optimum value of k_T may be found from Eqs. (78) and (80). The system time constant τ is then found from Eq. (19). Fig. 6 is a plot of these results and shows system time constant τ versus crossover loss in dB from Eq. (74) for selected values of T_s, and P_s in dBm. The dependence of τ on P is very weak and therefore a value of 30 seconds is selected as being satisfactory for all cases in practise. The value of AP equal to two seconds is also selected as being used in the current system (Ref. 1).

The values in Fig. 6 are actually the constraints imposed upon the conical-scan system by the weakness of the received signal. For example, if a 25^k receiver is to receive a signal at -175 dBm, with a system time constant less than 400 seconds, then the optimum crossover loss is 0.16 dB. Alternatively, if the crossover loss is constrained to be 0.10 dB, then the system time constant must be set to 950 seconds to avoid excessive jitter in the error offsets.

Setting the system time constant and crossover loss for a given weak signal, and then receiving a stronger signal will simply result in less error jitter if the proper procedure is followed. From Eqs. (11) and (64), it is seen that the system gain is proportional to the square root of the received signal power. Thus the system gain and hence the time constant τ should be adjusted for the actual signal strength being received. One method for such adjustment is to open the loop, put in a known offset ϕ and measure the average correlator output X_1. The value of k_i can then be found from Eq. (63). The values of k_T and τ are then found from Eqs. (11) and (19).

In the case of strong signal reception, the recommended parameters for conservative operation of the conical-scan system are a time constant of 90 seconds and a crossover loss of 0.09 dB. A much smaller time constant, or a lower crossover loss, might have a negative effect on the antenna mechanisms and increase jitter caused by imperfect mechanical

components. After selecting the desired values of τ and cross-over loss, C_L, the corresponding values of k_T and R may be found by inverting Eqs. (19) and (74).

$$k_T = 1 - \exp\left(-\frac{P}{\tau}\right) \tag{81}$$

$$R = W\left(\frac{C_L}{40 \log_{10} 2}\right)^{\frac{1}{2}} \tag{82}$$

Since Eq. (79) shows a fixed relationship exists between F and R, independent of T_s and P_s, the value of F in dB is also given in Fig. 6 as a horizontal scale beneath C_L according to an equation similar to Eq. (74).

$$F_{dB} = F^2\ 40 \log_{10} 2 \tag{83}$$

VI. Radio Source Tracking Correlation

A. Correlation Gain Constant

The development of equations for radio source tracking follows along lines similar to those for spacecraft tracking. Figure 7 is a simplified block diagram of the radio source tracking receiver system. Wide band energy from the radio source impinges upon the antenna with an equivalent noise temperature of T_r degrees. At point "e" of Fig. 7, the voltage $V_e(t)$ is random noise

$$V_e(t) = n_e(t) \tag{84}$$

with Φ_e, the two-sided spectral density of $n_e(t)$, being

$$\Phi_e(\omega) = \frac{KT_i}{2} \tag{85}$$

$$T_i = T_s + G_p T_r \tag{86}$$

where T_i is the total input temperature, T_s is the system temperature, and G_p is the antenna power gain defined in Eq. (34). $V_f(t)$, the voltage at point "f" in Fig. 7, is also random noise

$$V_f(t) = n_f(t) \tag{87}$$

$$\Phi_f(\omega) = \frac{H^2 KT_i}{2} \tag{88}$$

The two-sided spectral density Φ_f is band limited by the one-sided IF receiver bandwidth of B hertz. $V_g(t)$, the voltage at point "g" of Fig. 7, is formed by the squaring operation of the power detector

$$V_g(t) = E_g(t) + n_g(t) \tag{89}$$

$$E_g(t) = \alpha H^2 KT_i B \tag{90}$$

$$\Phi_g(0) = \alpha^2 H^4 K^2 T_i^2 B \tag{91}$$

where $E_g(t)$ is a DC voltage proportional to the input power, α is the power detector gain constant, $n_g(t)$ is a noise voltage riding on $E_g(t)$, and $\Phi_g(0)$ is the spectral density of $n_g(t)$ about zero frequency. High frequency terms from the squaring process are filtered out by a low pass filter internal to the power detector.

After each period P, the correlator output X_2 is

$$X_2 = X_1 + N \tag{92}$$

$$X_1 = k_c \int_{AP}^{P} dt\, E_g(t) \sin \omega_m t \tag{93}$$

$$N = k_c \int_{AP}^{P} dt\, n_g(t) \sin \omega_m t \tag{94}$$

Using Eqs. (34), (52), (54), (86), (90), and (93), X_1 is found to be

$$X_1 = -\, k_c \alpha H^2 KBP(1 - A)T_r \exp\left[-\frac{\mu}{W^2}(R^2 + \phi^2 + \theta^2)\right]$$

$$\times \frac{\phi}{\sqrt{\phi^2 + \theta^2}} I_1\left(\frac{2R\mu}{W^2}\sqrt{\phi^2 + \theta^2}\right) \tag{95}$$

For ϕ and θ much less than R, the approximation of Eq. (56) or of Eq. (57) may be used to linearize X_1

$$X_1 = - k_c \alpha H^2 K B P (1 - A) T_r \frac{R\mu}{W^2} \exp\left(- \frac{\mu R^2}{W^2}\right)\phi \quad (96)$$

Comparison with Eq. (63) gives the constant k_i

$$k_i = \frac{k_c \alpha H^2 K B T_r \mu}{W^2} \exp\left(- \frac{\mu R^2}{W^2}\right) \quad (97)$$

The S-curve constraint for larger values of ϕ is

$$y = - \frac{X_1 W \exp\left(\frac{\mu R^2}{W^2}\right)}{k_c \alpha H^2 K B P (1 - A) T_r R \mu} = \frac{\phi}{W} \exp\left[- \mu \left(\frac{\phi}{W}\right)^2\right] \quad (98)$$

and is also plotted in Fig. 5.

B. Radio Source Tracking Noise

The noise variance σ_N^2 is found by substituting Eq. (94) into Eq. (65) to give

$$\sigma_N^2 = k_c^2 \int_{AP}^{P} dt \int_{AP-t}^{P-t} d\tau_1 \, \beta_g(\tau_1)$$

$$\sin \omega_m t \sin \omega_m (t + \tau_1) \quad (99)$$

where $\beta_g(\tau_1)$ is the autocorrelation of $n_g(t)$ as a function of the lag time τ_1. Using the same reasoning as was done for spacecraft tracking, $\beta_g(\tau_1)$ is found to be

$$\beta_g(\tau_1) = \alpha^2 H^4 K^2 T_i^2 B \, \delta(\tau_1) \quad (100)$$

where T_i is now taken to be

$$T_i = T_s + \exp\left(- \frac{\mu R^2}{W^2}\right) T_r \quad (101)$$

Eqs. (99), (100), and (101) give

$$\sigma_N = k_c \alpha H^2 K \left(T_s + \exp\left[- \frac{\mu R^2}{W^2}\right] T_r\right) \sqrt{\frac{BP(1 - A)}{2}} \quad (102)$$

from which Eq. (31) becomes

$$\sigma_E = \frac{W^2 \left(T_s \exp\left[\frac{\mu R^2}{W^2}\right] + T_r\right)}{T_r R \mu \sqrt{2BP(1 - A)}} \sqrt{\frac{k_T}{2 - k_T}} \quad (103)$$

For normal radio star sources, the large value of B, typically 10^7 hertz, makes σ_E insignificant. Therefore the conservative parameters recommended for strong signal spacecraft tracking are also recommended for radio source tracking.

VII. Conclusion

The conical-scan tracking system has been analyzed in terms of a sampled-data feedback control system. This can facilitate further investigation into such questions as response to ramp inputs, and design of a higher order loop. Moreover, a rationale has been developed for selection of system parameters in both the spacecraft and radio source tracking modes. In the case of spacecraft tracking it is shown that reasonable tracking performance can be obtained at signal levels down to receiver threshold. Appendix A lists the symbols used in this report and the equations in which they first appear. Appendix B gives the correspondence between selected symbols of this report and symbols of Ref. 1.

References

1. Ohlson, J. E., and Reid, M. S., "Conical-Scan Tracking With the 64-m-diameter Antenna at Goldstone," Technical Report 32-1605, Jet Propulsion Laboratory, Pasadena, California, October 1, 1976.

2. Jury, E. I., *Theory and Application of the Z-Transform Method,* John Wiley & Sons, Inc., New York, 1964.

3. Mason, S. J., "Feedback Theory – Further Properties of Signal Flow Graphs," Proceedings of the Institute of Radio Engineers, Vol. 44, July 1956.

4. Nishimura, T., and Jury, E. I., "Contribution to Statistical Designing of Sampled-Data Control Systems," Electronics Research Laboratory Report Series 60, Issue No. 210, August 5, 1958, University of California, Berkeley.

5. Viterbi, A. J., *Principles of Coherent Communication,* McGraw-Hill Book Co., New York, 1966.

6. Gradshteyn, I. S., and Ryzhik, I. M., *Table of Integrals, Series, and Products,* #3.937, Academic Press, New York, 1965.

7. Davenport, W. B., and Root, W. L., *An Introduction to the Theory of Random Signals and Noise,* Appendix 1, McGraw-Hill Book Co., New York, 1958.

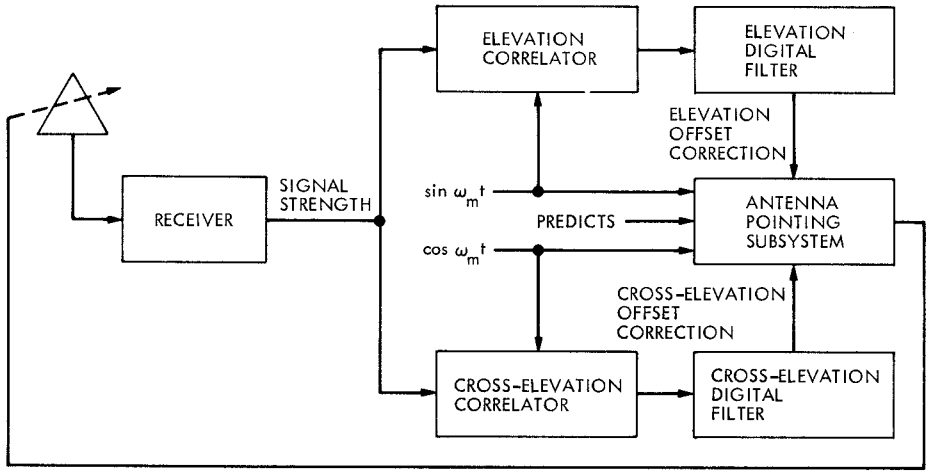

Fig. 1. System block diagram

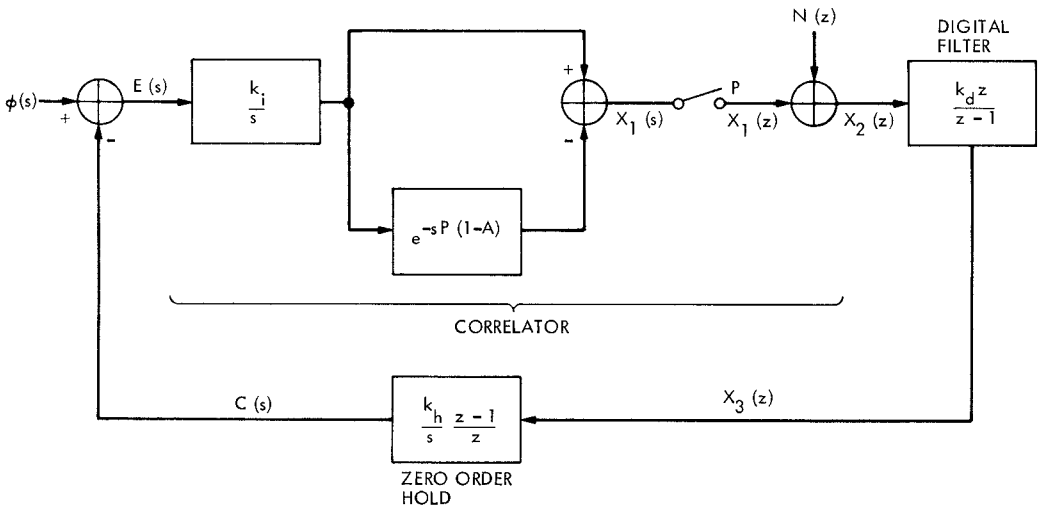

Fig. 2. Laplace block diagram

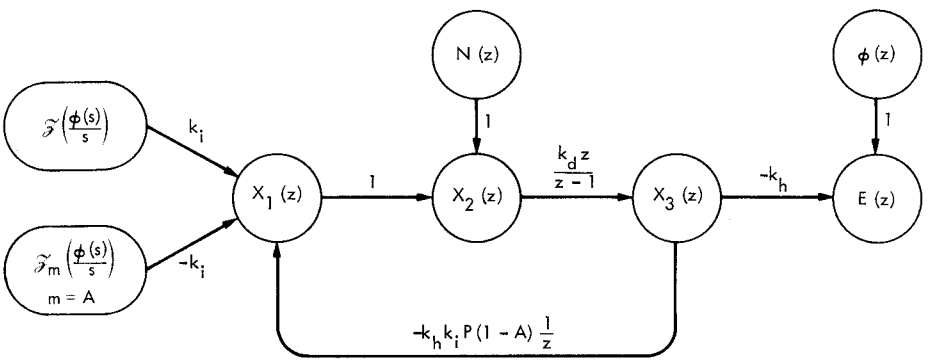

Fig. 3. Signal flow graph

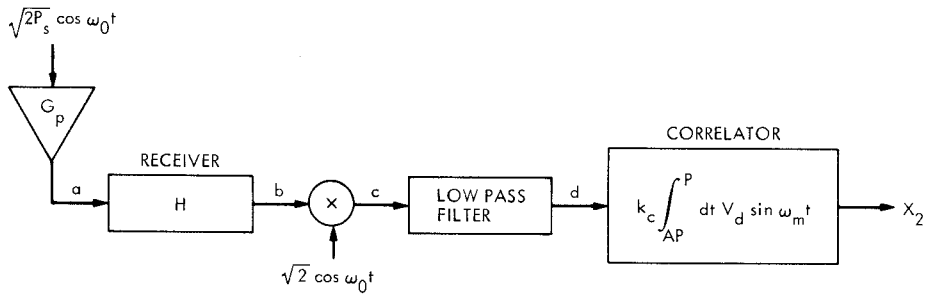

Fig. 4. Spacecraft tracking receiver system

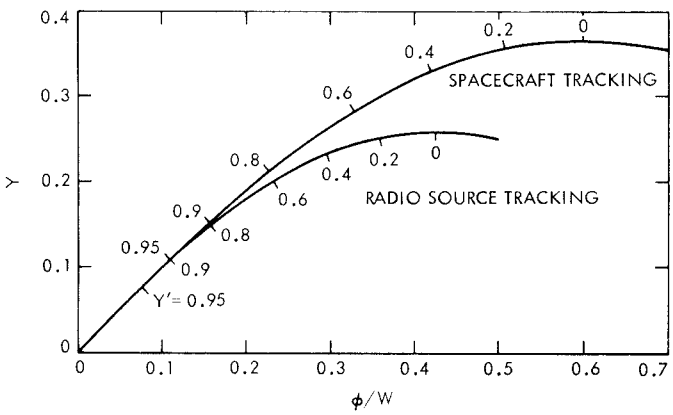

Fig. 5. Correlation S-curves

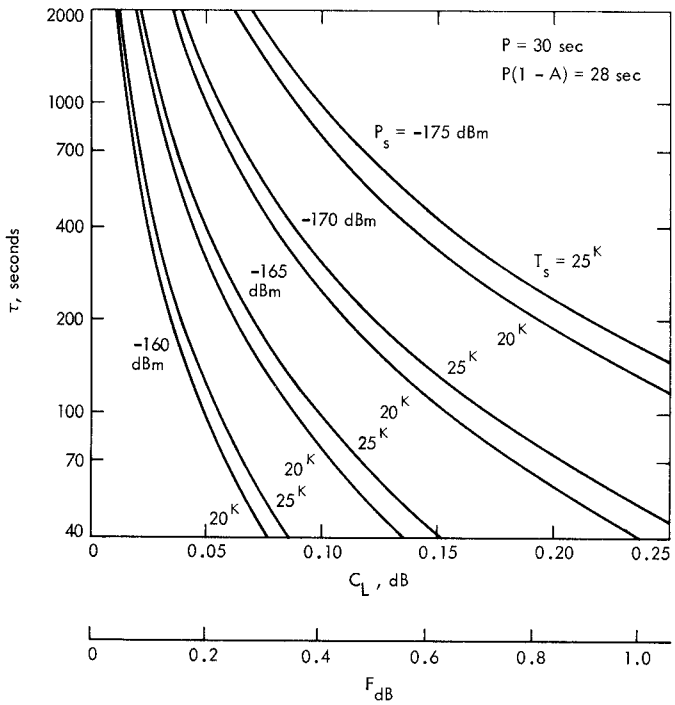

Fig. 6. Optimum conical-scan parameters for spacecraft tracking

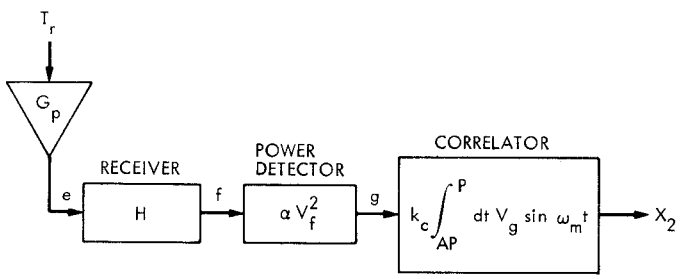

Fig. 7. Radio source tracking receiver system

Appendix A
List of Symbols

Following is a list of symbols used in this report and the equation number in which they first appear.

A	(1)	n_a	(36)	β_d	(66)
$C(s)$	(3)	n_b	(39)	β_E	(29)
C_L	(74)	n_c	(44)	β_g	(99)
D	(76)	n_d	(47)	β_N	(26)
$E(s)$	(3)	n_e	(84)	δ	(69)
$E(z)$	(8)	n_f	(87)	θ	(52)
E_a	(36)	n_g	(89)	μ	(34)
E_b	(39)	P	(1)	σ_E	(30)
E_c	(44)	P_s	(32)	σ_N	(26)
E_{ca}	(32)	R	(52)	τ	(18)
E_d	(47)	s	(3)	τ_1	(66)
E_g	(89)	T_i	(86)	ϕ	(52)
F	(75)	T_r	(86)	ϕ_c	(12)
F_{dB}	(83)	T_s	(38)	$\phi(s)$	(3)
G_{cl}	(22)	V_a	(36)	$\phi(z)$	(8)
G_{ol}	(20)	V_b	(39)	Φ_1	(43)
G_p	(33)	V_c	(44)	Φ_2	(43)
H	(40)	V_d	(47)	Φ_a	(38)
K	(38)	V_e	(84)	Φ_b	(41)
k	(2)	V_f	(87)	Φ_E	(24)
k_c	(50)	V_g	(89)	Φ_e	(85)
k_d	(2)	W	(33)	Φ_f	(88)
k_h	(5)	X_1	(5)	Φ_g	(91)
k_i	(5)	X_2	(2)	Φ_N	(24)
k_T	(11)	X_3	(2)	ω_m	(1)
N	(6)	Y	(73)	ω_0	(32)
n_1	(42)	z	(4)	ψ	(33)
n_2	(42)	α	(90)		

Appendix B

Correspondence With TR 32-1605

A correspondence is given between selected symbols of Technical Report 32-1605 and the equivalent symbol or expression in this report. Numbers in parentheses are the equation numbers in TR 32-1605 in which the symbols first appear.

TR 32-1605		This Report
A	(17)	$k_i P(1 - A)$
B	(11)	B
C	(11)	$k_c \quad H^2 K$
g	(10a)	G_p
h	(15)	$k_h k_d$
K	(73)	$k_c H$
k	(99)	K
N_O	(65)	KT_s
P	(15)	$P(1 - A)$
P_S	(61)	P_s
R	(1)	R
r	(27)	$1 - k_T$
T_i	(10a)	T_i
T_{OP}	(10a)	T_s
T_S	(10a)	T_r
W	(49)	W
β	(3)	ψ
ϕ	(2)	ϕ
σ_N	(22)	σ_N
σ_ϕ	(38)	σ_E
τ	(35)	τ
ω_m	(1)	ω_m